Quaternary International 400 (2016) 187–194

Contents lists available at ScienceDirect

Quaternary International

journal homepage: www.elsevier.com/locate/quaint

Pedostratigraphy of aeolian deposition near the Yunxian Man site on the Hanjiang River terraces, Yunxian Basin, central China

Xuefeng Sun [a, *], Yinghua Li [b], Xiaobo Feng [c], Chengqiu Lu [d], Huayu Lu [a], Shuangwen Yi [a], Shejiang Wang [e], Shuang-Ye Wu [a, f]

[a] School of Geographic and Oceanographic Sciences, Nanjing University, Nanjing 210023, China
[b] School of History, Wuhan University, Wuhan 430072, China
[c] College of Arts and Science, Beijing Union University, Beijing 100191, China
[d] Hubei Provincial Institute of Cultural Relics and Archaeology, Wuhan 430077, China
[e] Key Laboratory of Vertebrate Evolution and Human Origins of Chinese Academy of Sciences, Beijing, Institute of Vertebrate Paleontology and Paleoanthropology, Chinese Academy of Sciences, Beijing, 100044, China
[f] Geology Department, University of Dayton, Dayton, OH 45469-2364, USA

ARTICLE INFO

Article history:
Available online 19 June 2015

Keywords:
Yunxian Basin
Aeolian deposit
Terrace
Hominin occupation
Dating

ABSTRACT

Since 2010, we have found stone artifacts at the Houfang and Dishuiyan loess sections on the second terrace of the Hanjiang River and the Wolonggang thick natural loess section on the fifth terrace of the same river near the Xuetangliangzi site. We dated Dishuiyan and Houfang loess sections by optically stimulated luminescence (OSL) and thermally transferred OSL (TT-OSL) methods respectively. Dating results showed that the loess–paleosol deposited on the second Hanjiang River terrace as L1, S1, L2, and S2 in sequence. We dated the Wolonggang loess section by high-resolution paleomagnetostratigraphic analyses. The Jaramillo subchron was found at this section. Correlating with the central Loess Plateau, we recognized the continuous loess–paleosol sequence from L9 to L15. Investigations showed that loess was continuously deposited on the terraces of the Hanjiang River at Yunxian Basin since at least 1200 ka.

1. Introduction

Two fossil human crania show features associated with *Homo erectus* were successively discovered in the Xuetangliangzi (Yunxian Man) site at the Yunxian Basin, Hubei province, central China in 1989 and 1990 (Li and Etler, 1992, 1994; Li and Feng, 2001; Feng, 2004, 2008). The preliminary paleomagnetism dating suggested an age about 0.8 Ma (Yan, 1993). A later high-resolution magnetostratigraphic dating result put the age approximately at 0.9Ma (De Lumley and Li, 2008). A recent ESR dating showed a result of about 1.10 Ma (Feng et al., 2011). Until now, the pedostratigraphy study of the Xuetangliangzi site was limited, and the ages of the Yunxian Man and the Yunxian Paleolithic assemblages remained controversial.

At the Xuetangliangzi site, the deposition cover is only 7 m thick with only one loess unit and one paleosol complex. This caused problems in paleomagnetism dating and loess–paleosol sequence correlation with the central Loess Plateau. Furthermore, previous investigations regarded the widely distributed Quaternary deposits in Yunxian Basin as fluvial sediment (Huang and Li, 1995; De Lumley and Li, 2008).

Aeolian deposits are widely distributed in China (Liu, 1985). The Qinling Mountains are a natural barrier blocking the spread of dust from the north to the south. In the north, many thick aeolian depositions have been well studied (Liu, 1985; Liu and Ding, 1998; Ding et al., 1998, 2001; Lu et al., 1999, 2004). A small quantity of fine particle dust suspending at higher levels could cross over the Qinling Mountains (Yang et al., 1997; Han, 1988; Xiong et al., 2000, 2002; Qiao et al., 2003, 2011; Lu et al., 2008, 2011; Sun et al., 2012). Yunxian Basin is located south of the Qinling Mountains (Fig. 1).

Since 2010, during our field investigations in the Yunxian Basin, we found that the sediment cover in this area was aeolian. Stronger weathering and pedogensis processes were clear during the field observation. Aeolian silts were deposited on the Hanjing River terrace system with a thickness ranging from 2 to 30 m. There were some thick sections containing distinct loess–paleosol sequences near the Xuetangliangzi section. These aeolian sections could provide more information about the pedostratigraphy and ages of the

* Corresponding author.
E-mail address: xuefeng@nju.edu.cn (X. Sun).

http://dx.doi.org/10.1016/j.quaint.2015.05.034
1040-6182/

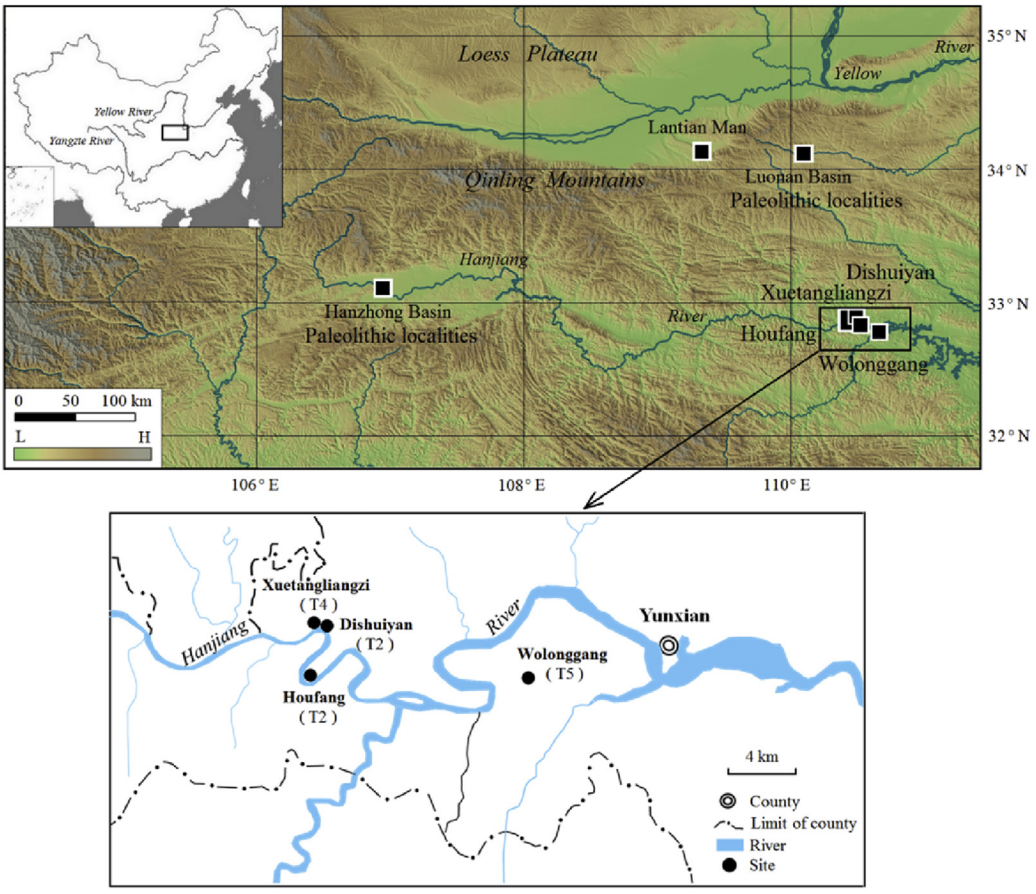

Fig. 1. Location of the Yunxian Man (Xuetangliangzi) site in the Yunxian Basin at the south Qinling Mountains and the Middle Pleistocene archaeological sites around the Qinling Mountains.

Yunxian Man and the Yunxian Paleolithic assemblages. Based on investigations of these aeolian sections from the first to the fifth terraces (Fig. 2), we could outline the pedostratigraphy of the aeolian deposition at the Yunxian Basin.

2. Geographical setting and sampling

Previous studies differentiated four Hanjiang River terraces in the Yunxian Basin (Shen et al., 1956; Huang and Li, 1995; De Lumley and Li, 2008). In 2012, we carried out detailed investigation and measurement on the Hanjiang River terrace system (Fig. 2). In this study, we identified six terraces near the Xuetangliangzi site, Yunxian Basin. The first terrace was found along both sides of the river. The fluvial cobbles occurred 5–10 m above the modern riverbed and the loess cover was about 5 m thick. The second terrace was also found on both the north and south banks, with most village buildings on it. The fluvial sand and cobbles occurred 20–25 m above the modern riverbed, and the aeolian deposit on top was less than 10 m thick. On the third terrace, the base of fluvial sand and cobbles was 40–45 m above the riverbed. The loess cover was very thin, less than 5 m. Some small villages were built on the third terrace. The fourth terrace was at 50–60 m above the current riverbed. The aeolian deposit on the fourth terrace was 5–10 m thick and contained a thin loess unit and a paleosol complex. The Xuetangliangzi site was on this terrace. The fifth terrace was 65–75 m above the riverbed and was covered by thick loess comprising indistinct loess–paleosol alternations. We also found a sixth terrace which was about 90 higher than the current riverbed. On the sixth terrace, fluvial pebbles were exposed on the bed rock.

In 2010, many stone artifacts were excavated by the team of Professor Li Yinghua at the Houfang site (Li and Sun, 2013). The Houfang site was only about 2 km away from the Xuetangliangzi site, about 187 m above sea level. It was on the second Hanjiang River terrace. We found a loess unit and two paleosol complexes at the Houfang loess section (Fig. 3). We took sediment samples for luminescence dating at the top, middle, and bottom of the section.

In 2012, numerous stone artifacts were excavated by the team of Professor Feng Xiaobo at the Dishuiyan site, which was adjacent to the Xuetangliangzi site (Liu and Feng, 2014). The Dishuiyan site was also on the second Hanjiang River terrace about 181 m above sea level. We found two loess layers and a paleosol unit at the Dishuiyan loess section. We took OSL samples from the top, the middle, and the bottom of the section.

In 2012, we found a thick natural loess section at the Wolonggang village (Fig. 3). This section contained distinct loess–paleosol alternations at about 230 m above sea level. The Wolonggang section was on the fifth Hanjing River terrace. It was 15.5 m thick and approximately 14 km from Xuetangliangzi section. During the field observation, we could easily make out the loess–paleosol sequence, which contained 8 loess units and 7 paleosol complexes (Fig. 3) based on changes of soil color. Loess units were light yellowish brown 10YR 6/4 and 10YR 6/6 (Munsell). Paleosol layers were brown 7.5YR 5/6 and strong brown 7.5YR 4/6. Loess units in southern China differ from those in northern China. They are closer to weakly developed soil (Sun et al., 2012; Zhang et al., 2012).

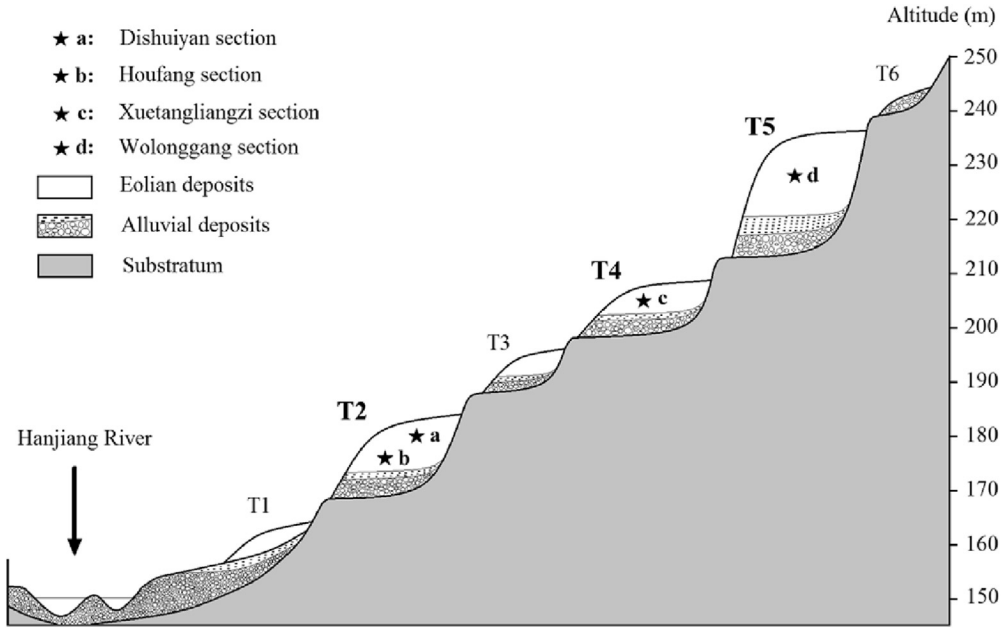

Fig. 2. Terrace system of the Hanjiang River and aeolian deposit at the Yuanxian Basin. The position of the Dishuiyan, Houfang, Wolonggang, and Xuetangliangzi sections are also shown.

Although we regarded the light color layer as loess at the Wolonggang section, they were actually weakly developed soil layers. We took paleomagnetism samples from the top to the bottom at the section. High resolution block samples were taken with the north direction marked on the top face for paleomagnetism dating at 10 cm intervals from 10 cm to 400 cm and at 20 cm intervals from 400 cm to 1600 cm at the Wolonggang section.

3. Methods

Optically stimulated luminescence (OSL) dating, using the single aliquot regeneration (SAR) protocol (Murray and Wintle, 2003) has been widely used for sedimentary grains (Murray and Wintle, 2000) particularly, in deserts and the Loess Plateau in China (Buylaert et al., 2007; Roberts, 2008; Lai, 2010). Thermally transferred optically stimulated luminescence (TT-OSL) (Wang et al., 2006, 2007; Tsukamoto et al., 2008; Stevens et al., 2009; Sun et al., 2013) has offered new approaches for establishing age control on sedimentary deposits that exceed the traditional upper age limits of quartz OSL dating. Magnetic polarity chronostratigraphy method is useful in establishing temporal control of loess deposition and hominin-bearing strata in north and central China (An and Ho, 1989; Zhu et al., 2001, 2004; Deng et al., 2008; Ao et al., 2012). In this study, we used OSL, TTT-OSL, and magnetic polarity chronostratigraphy methods to date the aeolian deposits in the Yunxian Basin.

4. Measurements

4.1. OSL measurements for the Houfang and Dishyian samples

The light-exposed ends of the sample tubes were removed in the laboratory under subdued red light and used for water content measurement and dose rate analysis. The unexposed material was then prepared for extraction of pure quartz grains. The samples

Fig. 3. Photos of Wolonggang section (16 m) form T5, Xuetangliangzi section (8 m) form T4, and Houfang-2 section (1.2 m) and Dishuiyan-2 section (1.5 m) from T2.

were first treated with 10% hydrochloric acid (HCl) and 30% hydrogen peroxide (H_2O_2), and then the 63–90 μm size fraction was extracted by wet sieving. After drying, the pure quartz (no significant IRSL signals) was obtained after a 40 min 40% hydrofluoric (HF) acid etch and 10% hydrochloric acid rinsing.

All measurements were carried out in the Luminescence Dating Laboratory at Nanjing University. All signals were measured using a Risø TL/OSL reader model DA-20equipped with a beta source calibrated for stainless steel discs. Blue LEDs ($\lambda = 470 \pm 30$ nm) were used for optical stimulation of the quartz grains. The quartz signals were measured using an EMI 9235QB15 photomultiplier tube and 7.5-mm-thick Hoya U–340 glass filter (Bøtter-Jensen et al., 1999). Quartz grains were mounted as large (8 mm diameter) aliquots on stainless steel discs.

The concentrations of ^{238}U, ^{232}Th and ^{40}K were obtained by neutron activation analysis (NAA). Sample-specific water contents were determined by laboratory analysis and the absolute uncertainty in the water content was assumed to be ±5% (Table 1). The cosmic ray dose rate was calculated using present–day burial depths (Prescott and Hutton, 1994). A summary of the dosimetry data for all samples is listed in Table 1.

After systematical thermal demagnetization, all results were evaluated by orthogonal diagrams (Zijderveld, 1967). The principal components direction was computed by a "least-squares fitting" technique (Kirschvink, 1980), using the KIRSCH software. The ChRM directions were then determined by using at least six continuous steps of demagnetization and with a maximum angular deviation (MAD) usually smaller than 15°. Most specimens (90%) gave reliable characteristic remanence directions. On the basis of these analyses, inclination and declination of all oriented samples were plotted in Fig. 5, and the virtual geomagnetic pole (VGP) latitudes were calculated from the ChRM data to construct the magnetostratigraphy for the Wolonggang section (Fig. 6).

5. Results

5.1. Equivalent dose (D_e) determination, OSL age, and TT-OSL age results

Initially, the SAR protocol proposed by Murray and Wintle (2000, 2003) was used to determine the sample equivalent doses. The initial 0.16 s of the OSL signal minus an early background (0.16–0.32 s) was used for the calculation. Dose response curves were fitted using saturating exponential or saturating exponential plus linear functions in Analyst version 4.11. Aliquots with $2 \times D_0$ values smaller than the dose we are trying to measure (derived from all aliquots) are not incorporated in the final De calculation, irrespective of the De value of the individual aliquot. This criterion is used to ensure that only those aliquots that are capable of measuring the dose of interest are included in the calculation of the mean D_e. For DSY-T, DSY-M, and DSY-B, this criterion leads to a rejection rate as, of 0%, 8.3%, and 42% respectively. For all samples, recuperation was <3% and the average recycling ratio is 1.001 ± 0.003 indicating that the adopted SAR protocol successfully corrects for sensitivity changes. The OSL signals decreased very quickly during the first second of stimulation. The D_e and dose rate information of the Dishuiyan section are listed in Table 1. The OSL D_e values ranges from 87 ± 7 to 252 ± 17 Gy. OSL ages ranged from 25 ± 2 ka to 108 ± 9 ka (Table 1). Typical dose response curves and OSL decay curves are shown for DSY-B samples in Fig. 4a.

At the Houfang site, the OSL measurements were saturated. Then the TT-OSL equivalent measurements were carried out using the protocol proposed by Stevens et al. (2009). The TT-OSL signal was calculated from the sum of the first 0.6 s of optical stimulation, from which a background signal was subtracted, estimated from the final 6 s of optical stimulation (total stimulation time 60 s). The recuperation values were less than 10% in all cases. The recycling ratios of these samples ranged between 0.91 ± 0.17 (n = 8; HF-T) to 1.15 ± 0.14 (n = 10; HF-B). Dose response curves were fitted using saturating exponential or saturating exponential plus linear functions. A representative TT-OSL decay curve and the

Table 1
Radioactive data, water content, equivalent dose, dose rate, OSL, and TT-OSL ages of the samples from the Dishuiyan (DSY) section and the Houfang (HF) section.

Sample no.	Depth	U (ppm)	Th (ppm)	K (%)	H_2O (%)	De (Gy)		Dose rate (Gy/ka)	Age (ka)	
						OSL	TT-OSL		OSL	TT-OSL
DSY-T	Top	2.38 ± 0.09	14.9 ± 0.40	2.28 ± 0.07	15	87.1 ± 6.9		3.15 ± 0.16	24.9 ± 2.4	
DSY-M	Middle	2.33 ± 0.09	14.4 ± 0.39	2.25 ± 0.07	15	158.1 ± 8.2		3.43 ± 0.18	45.2 ± 3.3	
DSY-B	Bottom	2.18 ± 0.09	8.95 ± 0.28	1.43 ± 0.05	15	251.9 ± 16.8		3.37 ± 0.17	108.1 ± 9.1	
HF-T	Top	3.11 ± 0.11	14.9 ± 0.40	2.09 ± 0.06	15		316.0 ± 25.7	3.70 ± 0.18		85.3 ± 8.3
HF-M	Middle	2.61 ± 0.10	14.6 ± 0.39	2.04 ± 0.06	15		512.3 ± 17.0	3.43 ± 0.17		149.2 ± 9.4
HF-B	Bottom	2.79 ± 0.10	13.9 ± 0.36	1.86 ± 0.06	15		607.2 ± 37.7	3.27 ± 0.23		185.5 ± 17.3

4.2. Paleomagnetic measurements for the Wolonggang samples

Paleomagnetic measurements were performed in the Nanjing University. Blocks were cut into cubic specimens (approximate $2 \times 2 \times 2$ cm^3) with a non-magnetic saw. Remanence measurements were made using a 2G Enterprises Model 760R cryogenic magnetometer undertaken at room temperature. Samples were subjected to progressive thermal demagnetization using a magnetic measurements thermal demagnetizer. The progressive demagnetization successfully isolated characteristic remnant magnetization (ChRM) component after removing a viscous component of magnetization.

Initially, a suite of eight samples with good stratigraphic distribution were picked from the Wolonggang section for thermal demagnetization studies. All samples were subjected to progressive thermal demagnetization (12–16 steps) up to a maximum temperature of 680 °C (or 650 °C), with 50 °C interval below 500 °C, and 30 °C or 20 °C interval above 500 °C. All samples displayed demagnetization of a single direction toward the origin above 150–300 °C. That direction was usually lost by 550 °C, but a few samples had a considerable component of the same direction that demagnetized above 650 °C. No sample produced stable direction (stable end point) or directional loss above 680 °C. The pattern of intensity loss under thermal demagnetization (blocking temperature spectrum with most NRM loss by 550 °C or 650 °C) was largely consistent with the magnetite or hematite mineralogy respectively. On the basis of these measurements, all other samples in this study were subjected to thermal demagnetization up to 680 °C, with 50 C° intervals below 500 °C, and 30 C° or 20 C° intervals above 500 °C.

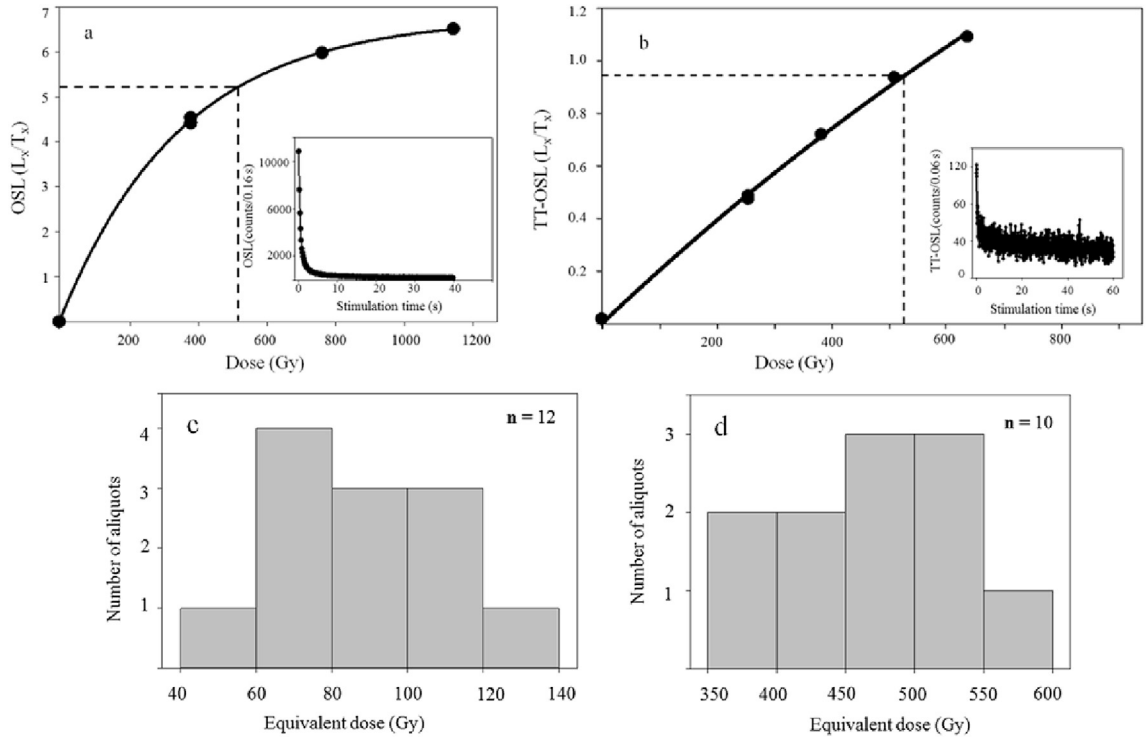

Fig. 4. Dose response and decay curves for Quartz SAR OSL form DSY-B (a) and for TT-OSL from HF-M (b). Frequency histogram of De distribution for DSY-T (c) and HF-M (d) from 12 to 9 single aliquots measurements respectively.

growth curve for one aliquot from sample HF-M is shown in Fig. 4b. Frequency histogram of D_e distribution for DSY-T (c) and HF-M (d) from 12 to 10 single aliquots measurements respectively were also shown in Fig. 4c and d. For all samples, the TT-OSL dose response curves were similar and showed D_e values between 316 ± 26 and 607 ± 38 Gy. The age ranged from 85 ± 8 ka to 186 ± 17 ka (Table 1). The low TT-OSL signal intensity (Fig. 4b) could lead to inaccuracy of the TT-OSL results.

5.2. Paleomagnetic results

Using demagnetization, three magnetozones were recognized at the Wolonggang section: two main reverses, R1 (0–230 cm) and R2 (280–1550 cm); and a small normal magnetozone, N1 (240–270 cm) (Fig. 6). However, on the basis of the paleomagnetic and sedimentological data, the magnetozones correlation between the Wolonggang and the geomagnetic polarity time scale (GPTS) (Cande and Kent, 1995; Ogg, 2012) was uncertain. However, Jaramillo and Olduvai excursions are two typical episodes between Brunhes chron and Gauss chron on the central Loess Plateau (Liu, 1985; Liu et al., 2010). These two subchrons are also well documented in Lantian Basin (Zheng et al., 1992; Wu et al., 2011) which is about 200 km away from the Yunxian Basin. From this, we inferred that the small normal magnetozone at the 240–270 cm in the Wolonggang section might be Jaramillo or Olduvai subchron.

Based on the normal magnetozone in depth 240–270 cm, it was reasonable to assume that the four paleosol complexes from 0 cm to 430 cm corresponded to S9, S10, S11, and S12 of the central Loess Plateau, and that the small normal magnetozone corresponded to the Jaramillo excursion. A paleosol layer at the depth of 620–700 cm corresponded to S13, and the paleosol complex at the depth of 850–900 cm with a calcium carbonate layer was S14. The thick sandy loess layer from 905 to 1550 cm corresponded to the loess unit L15 on the central Loess Plateau, also known as 'the lower sandy loess', a widely used stratigraphic marker (Fig. 6).

6. Discussion

6.1. Pedostratigraphy of aeolian deposition

At the Dishuiyan section, we found two loess layers and a paleosol unit. According to OSL ages (ranging from 25 ± 2 ka to 108 ± 9 ka) and correlation with loess–paleosol sequence on the central Loess Plateau (Lu et al., 1999; Heslop et al., 2000), the pedostratigraphy of the Dishuiyan loess section was recognized as L1, S1, and L2 in sequence. At the Houfang section, we found a loess unit and two paleosol complexes. According to TT-OSL ages (ranging from 85 ± 8 ka to 186 ± 17 ka) and correlation with loess–paleosol sequence on the central Loess Plateau (Lu et al., 1999; Heslop et al., 2000), the pedostratigraphy of the Houfang loess section was recognized as S1, L2, and S2 in sequence. The pedostratigraphy of the loess section at the second Hanjiang River terrace was L1, S1, L2, and S2 in sequence.

Several loess sections on the first Hanjiang River terrace were dated by OSL (Pang et al., 2014). Dating showed that the first Hanjing River terrace was formed since 25 ka. Correlation with the loess–paleosol sequence on the central Loess Plateau, the pedostratigraphy on the first Hanjiang River terrace was recognized as L0, S0, and L1 in sequence. Therefore, the dust sediment was continuous as L0, S0, L1, S1, L2, and S2 in sequence on the first and the second terrace.

At the Xuetangliangzi section on the fourth Hanjiang River terrace, a paleosol complex and a loess unit were regarded as S8 and L9 (Guo et al., 2013). The Wolonggang section on the fifth Hanjiang River terrace was dated by high-resolution paleomagnetostratigraphic analyses and correlation with the central Loess Plateau. We found a continuous loess–paleosol sequence

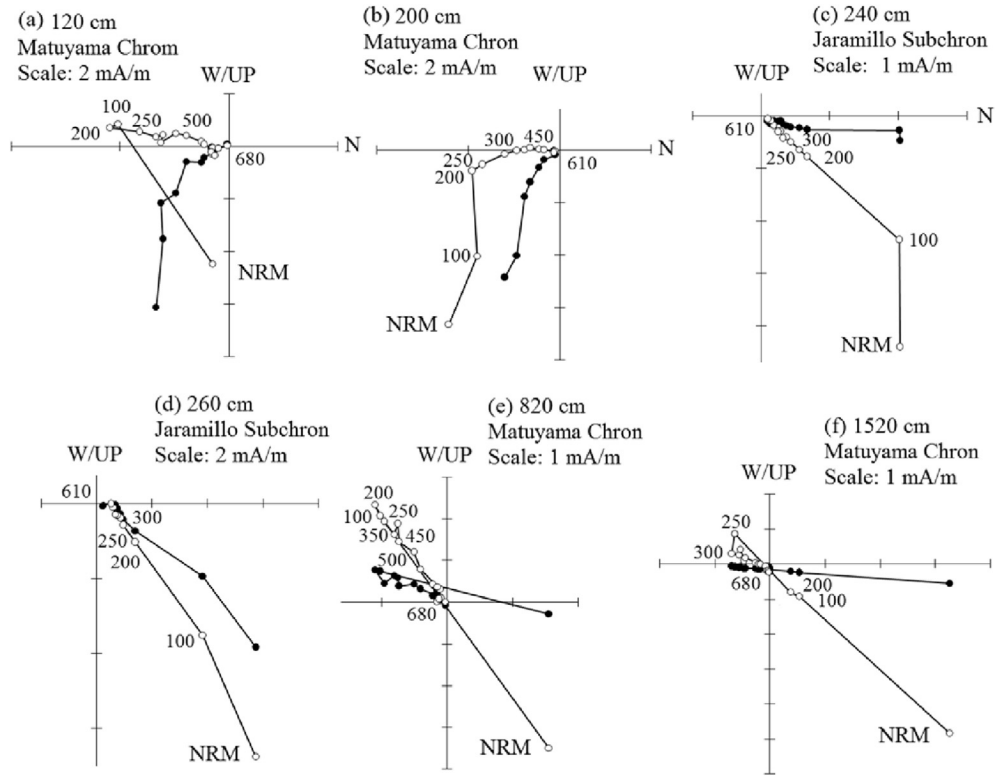

Fig. 5. Representative vector-end plots for progressive thermal demagnetization of selected samples from the Wolonggang section. Open and closed circles indicate projections onto the vertical and horizontal planes respectively. Numbers on the plots indicate heating temperatures in °C.

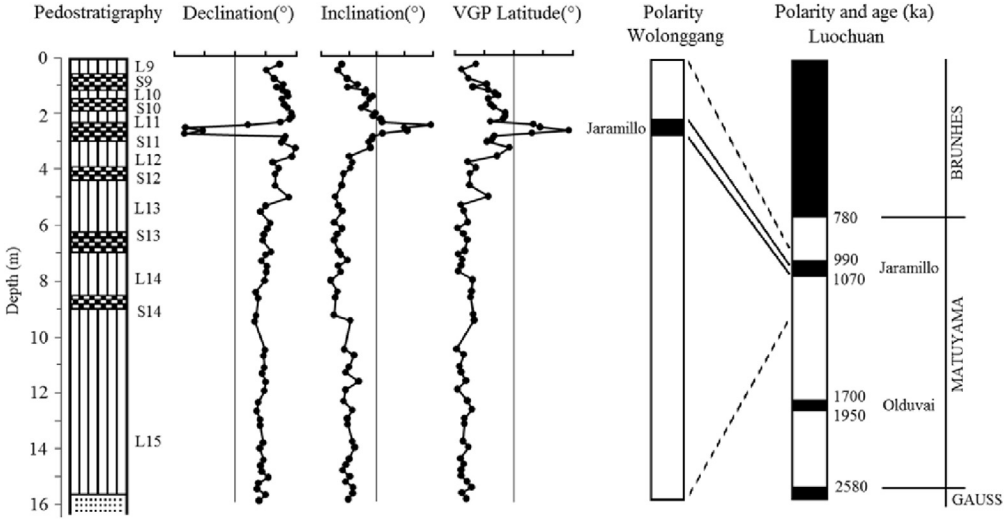

Fig. 6. Pedostratigraphy of the Wolonggang section, showing correlations between loess–paleosol sequence, declination, inclination, virtual geomagnetic pole (VGP) latitude, magnetic polarity zonation, and the geomagnetic polarity time scale of the standard Luochuan section.

from L9 to L15. Dust sediment was continuous as S8, L9, S9, L10, S10, L11, S11, L12, S12, L13, S13, L14, S14 and L15 in sequence at the fourth and the fifth terrace. Therefore, we concluded that loess–paleosol sequences are continuously distributed from the fifth to the first Hanjiang River terrace. On the higher terraces, the loess sediment was old and at the lower terraces the loess deposit was young. Furthermore, we believe that the break of dust sediment from L3 to L8 stages should be found on the third Hanjing River terrace during future investigations.

6.2. Glacial and interglacial paleoenvironmental changes at the Yunxian Basin

Loess deposits are important terrestrial records of environmental changes. The loess–soil sequences in southern China are valuable geological records of Quaternary environmental and climate change (Liu, 1985). In the Yunxian Basin, the loess–paleosol sequence at the Dishuiyan, Houfang, Xuetangliangzi, and Wolonggang sections recorded climate information of the glacial and interglacial periods.

At the fifth Hanjiang River terrace, the thick L15, L14, and L13 stages were formed under significantly strengthened winter monsoon. Thin S14 and S13 stages indicated weakened summer monsoon. At the fourth Hanjiang River terrace during L9 and S8 stages, both summer and winter monsoons were strengthened.

The increase of both dust sedimentation rate and grain size of the wind-blown silt deposit in northern China indicates a significant drying in central Asia (Lu et al., 2008, 2010). Equally, the onset and significant increase of dust in southern China was also the mark of paleoenvironmental drying. In the Yunxian Basin, the first onset of the aeolian deposit was located on the fifth terrace at Wolonggang section during MIS 34 (L15). The second significant increase of dust deposit was at the Xuetangliangzi section during MIS-22 (L9) at the fourth terrace. During MIS-34 and MIS-22, with the strengthening of the winter monsoon circulations, the paleoenvironment was dry. These two drying events in the Yunxian Basin were a response to the well-known Mid-Pleistocene climate change of global significance.

Intermountain basins at the south and east of Qinling Mountains had a relatively warm and humid climate during glacial periods of the Middle Pleistocene (Zhang et al., 2012). Mammalian fossil analysis (Feng et al., 2011) showed that during MIS-22 interglacial (L9), the paleoenvironment in the Yunxian Basin was still a subtropical warm-temperate climate with dense forest mixed with little grass. Therefore, we concluded that from L15 to L9, the paleoenvironment in the Yunxian Basin was still warm and humid. The climate was drier and cooler during the glacial periods than in interglacial periods. Hominins also lived during L9 (Li and Elter, 1992, Li et al., 1994; Li and Feng, 2001; Guo et al., 2013), L2 (Li and Sun, 2013; Li et al., 2014), and L1 (Liu and Feng, 2014) glacial stages at the Yunxian Basin.

7. Conclusions

According to our investigations at the Yunxian Basin, aeolian dust covered the fifth terrace since about 1200 to 900 ka, was deposited on the fourth terrace from approximately 1000 to 700 ka, on the second terrace from at least 190 to 24 ka, and covered the first terrace since at least 25 ka. The loess–paleosol sequences from the fifth to first Hanjiang River terrace should be continuous. The loess–paleosol sequences recorded the glacial and interglacial paleoenvironmental changes and hominin activities at the Yunxian Basin. Hominins occupied Yunxian Basin during two stages, from about 1000 to 780 ka at Xuetangliangzi site and from approximately 150 to 50 ka at Houfang and Dishuiyan sites.

Acknowledgements

We thank Langping Li, Guanjun Shen, Hua Tu, Yali Zhou, Xiaoyong Wang for valuable discussions. Thanks also go to Professors Gao Xing and Wei Wang for their encouragement and helpful discussions. This research was supported by the National Natural Science Foundation of China (41202127 and 41472026), specialized Research Fund for the Doctoral Program of Higher Education (20130091130006), the Priority Academic Program Development of Jiangsu Higher Education Institutions, the Fundamental Research Funds for the Central Universities, the Importation and Development of High-Caliber Talents Project of Beijing Municipal Institutions (CIT & TCD20140312), and the National Social Science Foundation of China (12BKG002).

References

An, Z.S., Ho, C.K., 1989. New magnetostratigraphic dates of Lantian Homo erectus. Quaternary Research 32, 213–221.

Ao, H., An, Z.S., Dekkers, M.J., Wei, Q., Pei, S.W., Zhao, H., Zhao, H.L., Xiao, G.Q., Qiang, X.K., Wu, D.C., Chang, H., 2012. High-resolution record of geomagnetic excursions in the Matuyama chron constrains the ages of the Feiliang and Lanpo Paleolithic sites in the Nihewan Basin, North China. Geochemistry Geophysics Geosystems 13.

Bøtter-Jensen, L., Mejdahl, V., Murray, A.S., 1999. New light on OSL. Quaternary Science Reviews 18, 303–309.

Buylaert, J.P., Vandenberghe, D., Murray, A.S., Huot, S., De Corte, F., Van den haute, P., 2007. Luminescence dating of old (>70 ka) Chinese loess: a comparison of single-aliquot OSL and IRSL techniques. Quaternary Geochronology 5, 9–14.

Cande, S.C., Kent, D.V., 1995. Revised calibration of the geomagnetic polarity timescale for the Late Cretaceous and Cenozoic. Journal of Geophysical Research 100 (B4), 6093–6095.

De Lumley, H., Li, T.Y., 2008. Le site de l'Homme de Yunxian: Quyuanhekou, Quingqu, Yunxian, Province Du Hubei. CNRS, Paris.

Ding, Z.L., Sun, J.M., Yang, S.L., Liu, T.S., 1998. Preliminary magnetostratigraphy of a thick aeolian red clay–loess sequence at Lingtai, the Chinese Loess Plateau. Geophysical Research Letters 25, 1225–1228.

Ding, Z.L., Sun, J.M., Yang, S.L., Liu, T.S., 2001. Geochemistry of the Pliocene red clay formation in the Chinese Loess Plateau and implications for its origin, source provenance and paleoclimate change. Geochimica et Cosmochimica Acta 65 (6), 901–913.

Deng, C.L., Zhu, R.X., Zhang, R., Ao, H., Pan, Y.X., 2008. Timing of the Nihewan formation and faunas. Quaternary Research 69, 77–90.

Feng, X.B., 2004. A study of the cores from the Yunxian Hominid site. Acta Anthropologica Sinica 23, 1–12 (in Chinese with English abstract).

Feng, X.B., 2008. Technological characterization of China and Europe lower Paleolithic industry from 1 Ma to 400,000 years Similarity and difference between the Yunxian Hominid culture and European Acheulean. L'anthropologie 112, 423–447.

Feng, X.B., Lu, C.Q., Wang, H., 2011. New advance in the study of the Homo erectus site in Yunxian County in Hubei. Jianghan Archaeology 120, 57–64 (in Chinese with English abstract).

Guo, Y., Huang, C.C., Pang, J., Zha, X., Zhou, Y., Zhang, Y., Zhou, L., 2013. Sedimentological study of the stratigraphy at the site of *Homo erectus* yunxianensis in the upper Hanjiang River valley, China. Quaternary International 300, 75–82.

Han, X.B., 1988. Depositional environment and age of Xiashu loess in Nanjing area. Contribution to the Quaternary Glaciolohy and Quaternary Geology (5) (eds. Commission on Quaternary Glaciology and Geology of the Geological Society of China, Geological Society of Jiangsu Province). Geological Publishing House, Beijing, pp. 56–62 (in Chinese).

Heslop, D., Langereis, C.G., Dekkers, M.J., 2000. A new astronomical timescale for the loess deposits of Northern China. Earth and Planetary Science Letters 184, 125–139.

Huang, P.H., Li, W.S., 1995. Landscape, Quaternary strata and buried environment at estuary of the Quyuan River in Yunxian County, Hubei Province. Jianghan Archaeology 4, 83–86 (in Chinese).

Kirschvink, J.L., 1980. The least-square line and plane and the analysis of aleomagnetic data. Geophysical Journal of the Royal Astronomical Society 62, 699–718.

Lai, Z.P., 2010. Chronology and the upper dating limit for loess samples from Luochuan section in the Chinese Loess Plateau using quartz OSL SAR protocol. Journal of Asian Earth Sciences 37, 176–185.

Li, Y.H., Sun, X.F., 2013. A preliminary report on the excavation at the Houfang Paleolithic site at Yun County, Hubei Province. Jianghan Archaeology 126, 6–15 (in Chinese with English abstract).

Li, Y.H., Sun, X.F., Bodin, E., 2014. A macroscopic technological perspective on lithic production from the Early to Late Pleistocene in the Hanshui River Valley, central China. Quaternary International 347, 148–162.

Li, T.Y., Etler, D.A., 1992. New Middle Pleistocene Hominid crania from Yunxian in China. Nature 357, 404–407.

Li, T.Y., Wang, Z.H., Li, W.S., Feng, X.B., Wu, X.Z., 1994. Morphological features of human skulls from Quyuan river mouth, Yunxian, Hubei and their place in human evolution. Acta Anthropologica Sinica 13 (2), 104–115 (in Chinese).

Li, T.Y., Feng, X.B. (Eds.), 2001. Yunxian Man. Science and Technique Press, Hubei, 218 pp (in Chinese with English abstract).

Liu, T.S., 1985. Loess and the Environment. Science Press, Beijing.

Liu, T.S., Ding, Z.L., 1998. Chinese loess and the paleomonsoon. Annual Review of Earth and Planetary Sciences 26, 111–145.

Liu, W.M., Zhang, L.Y., Sun, J.M., 2010. High resolution magnetostratigraphy of the Luochuan loess-paleosol sequence in the central Chinese Loess Plateau. Chinses Journal of Geophysics 53 (4), 888–894.

Liu, Y., Feng, X.B., 2014. The discovery of hand-axe with age between 0.05 and 0.10 Ma at Dishuiyan site, Hubei province. China Cultural Heritage Report 8, 1 (in Chinese).

Lu, H.Y., Liu, X.D., Zhang, F.Q., An, Z.S., Dodson, J., 1999. Astronomical calibration of loess-paleosol deposits at Luochuan, central Chinese Loess Plateau. Paleogeography, Paleoclimatology, Paleoecology 154, 237–246.

Lu, H.Y., Zhang, F.Q., Liu, X.D., Duce, R., 2004. Periodicities of paleoclimatic variations recoded by the loess-paleosol sequences in China. Quaternary Science Reviews 23, 1891–1900.

Lu, H.Y., Wang, X.Y., Li, L.P., 2008. Aeolian dust records indicate the linkage of global cooling and Asian drying in late Cenozoic. Quaternary Science 28, 949–956 (in Chinese with English abstract).

Lu, H.Y., Wang, X.Y., Li, L.P., 2010. Aeolian sediment evidence that global cooling has driven late Cenozoic stepwise aridification in central Asia. In: Clift, P.D., Tada, R., Zheng, H. (Eds.), Monsoon Evolution and Tectonics–Climate Linkage in Asia, Special Publications, 342. Geological Society, London, pp. 29–44.

Lu, H.Y., Zhang, H.Y., Wang, S.J., Cosgrove, R., Sun, X.F., Zhao, J., Sun, D.H., Zhao, C.F., Shen, C., Wei, M., 2011. Multiphase timing of hominin occupations and the paleoenvironment in Luonan Basin, Central China. Quaternary Research 76, 142–147.
Murray, A.S., Wintle, A.G., 2000. Luminescence dating of quartz using an improved single-aliquot regenerative-dose protocol. Radiation Measurements 32, 57–73.
Murray, A.S., Wintle, A.G., 2003. The single aliquot regenerative dose protocol: potential for improvements in reliability. Radiation Measurements 37, 377–381.
Ogg, J.G., 2012. Chapter 5: geomagnetic polarity time scale. In: Gradstein, F.M., Ogg, J.G., Schmitz, M.D., Ogg, G.M. (Eds.), The Geologic Time Scale 2012. Elsevier, Amsterdam, pp. 85–113.
Pang, J.L., Hang, C.C., Zhou, Y.L., Zha, X.C., Qiao, J., Zhang, Y.Z., Zhou, L., 2014. Formation of the first River Terraces of Hanjiang River and its response to the East Asian Monsoon change. Geological Review 60 (5), 1076–1084.
Prescott, J.R., Hutton, J.T., 1994. Cosmic ray contributions to dose rates for luminescence and ESR dating: large depths and long term variations. Radiation Measurements 23, 497–500.
Qiao, Y.S., Guo, Z.T., Hao, Q.Z., Wu, W.X., Jiang, W.Y., Yuan, B.Y., 2003. Loess–soil sequences in southern Anhui Province: magnetostratigraphy and paleoclimatic significance. Chinese Science Bulletin 48 (19), 2088–2093.
Qiao, Y., Hao, Q., Peng, S., Wang, Y., Li, J., Liu, Z., 2011. Geochemical characteristics of the aeolian deposits in southern China, and their implications for provenance and weathering intensity. Palaeogeography, Palaeoclimatology, Palaeoecology 308, 513–523.
Roberts, H.M., 2008. The development and application of luminescence dating to loess deposits: a perspective on the past, present and future. Boreas 37, 483–507.
Shen, Y.C., 1956. Geomorphology of the Hanshui Valley. Acta Geographica Sinica 4, 295–323 (in Chinese with English abstract).
Stevens, T., Buylaert, J.-P., Murray, A.S., 2009. Towards development of a broadly-applicable SAR TT-OSL dating protocol for quartz. Radiation Measurements 44, 639–645.
Sun, X.F., Lu, H.Y., Wang, S.J., Yi, S.W., 2012. Ages of Liangshan Paleolithic sites in Hanzhong Basin, central China. Quaternary Geochronology 10, 380–386.
Sun, X.F., Lu, H.Y., Wang, S.J., Yi, S.W., Shen, C., Zhang, W.C., 2013. TT-OSL dating of Longyadong Middle Paleolithic site and paleoenvironmental implications for hominin occupation in Luonan Basin (central China). Quaternary Research 79, 168–174.
Tsukamoto, S., Duller, G.A.T., Wintle, A.G., 2008. Characteristics of thermally transferred optically stimulated luminescence (TT-OSL) in quartz and its potential for dating sediments. Radiation Measurements 43, 1204–1218.
Wang, X.L., Lu, Y.C., Wintle, A.G., 2006. Recuperated OSL dating of fine-grained quartz in Chinese loess. Quaternary Geochronology 1, 89–100.
Wang, X.L., Wintle, A.G., Lu, Y.C., 2007. Testing a single-aliquot protocol for recuperated OSL dating. Radiation Measurements 42, 380–391.
Wu, Y., Zhu, Z.Y., Qiu, S.F., 2011. Review on magnetostratigraphic research of the Quaternary loess-paleosol sequence in the Lantian Basin. Progress in Geophysics 26 (1), 138–146 (in Chinese with English abstract).
Xiong, S.F., Ding, Z.L., Liu, T.S., 2000. The worm-shaped veins in the red earth of South China- Pedological evidence for root traces of past forest. Chinese Science Bulletin 45 (19), 1800–1804.
Xiong, S.F., Sun, D.H., Ding, Z.L., 2002. Aeolian origin of the red earth in southeast China. Quaternary Sciences 17 (2), 181–191.
Yan, G.L., 1993. A preliminary study on magnetic stratigraphy of the geological section with the fossil bed of Yunxian Homo of Hubei. Earth Science- Journal of China University of Geosciences 18 (2), 221–226.
Yang, D.Y., Li, X.S., Lu, H.Y., Han, H.Y., Ren, L.X., Fang, Y.S., 1997. Loess in Xuancheng prefecture of Anhui province and palaeolithic culture. Journal of Geomechanics 3 (4), 85–89 (in Chinese with English abstract).
Zijderveld, J.D.A., 1967. A.C. demagnetization of rocks: analysis of results. In: Collinson, D.W., Creer, K.M., Runcorn, S.K. (Eds.), Methods in Paleomagnetism. Elsevier, New York, pp. 254–286.
Zhang, H.Y., Lu, H.Y., Jiang, S.Y., Vandenberghe, J., Wang, S.J., Cosgrove, R., 2012. Provenance of loess deposits in the Eastern Qinling Mountains (central China) and their implications for the paleoenvironment. Quaternary Science Reviews 43, 94–102.
Zheng, H.B., An, Z.S., Shaw, J., 1992. New contributions to Chinese Plio- Pleistocene magnetostratigraphy. Physics of the Earth and Planetary Interiors 70, 146–153.
Zhu, R.X., Hoffman, K.A., Potts, R., Deng, C.L., Pan, Y.X., Guo, B., Shi, C.D., Guo, Z.T., Yuan, B.Y., Hou, Y.M., Huang, W.W., 2001. Earliest presence of humans in northeast Asia. Nature 413, 413–417.
Zhu, R.X., Potts, R., Xie, F., Hoffman, K.A., Deng, C.L., Shi, C.D., Pan, Y.X., Wang, H.Q., Shi, R.P., Wang, Y.C., Shi, G.H., Wu, N.Q., 2004. New evidence on the earliest human presence at high northern latitudes in northeast Asia. Nature 431, 559–562.